Grazing-sliding bifurcations, border collision maps and the curse of dimensionality for piecewise smooth bifurcation theory

Paul Glendinning

School of Mathematics, University of Manchester, Manchester M13 9PL, U.K.

E-mail: `p.a.glendinning@manchester.ac.uk`

Mike R. Jeffrey

Department of Engineering Mathematics, University of Bristol, Bristol BS8 1UB, U.K.

E-mail: `mike.jeffrey@bristol.ac.uk`

Abstract. We show that maps describing border collision bifurcations (continuous but non-differentiable discrete time maps) are subject to a curse of dimensionality: it is impossible to reduce the study of the general case to low dimensions, since in every dimension the bifurcation can produce fundamentally different attractors (contrary to the case of local bifurcations in smooth systems). In particular we show that n-dimensional border collision bifurcations can have invariant sets of dimension k for integer k from 0 to n. We also show that the border collision normal form is related to grazing-sliding bifurcations of switching dynamical systems. This implies that the dynamics of these two apparently distinct bifurcations (one for discrete time dynamics, the other for continuous time dynamics) are closely related and hence that a similar curse of dimensionality holds in grazing-sliding bifurcations.

1. Introduction

Despite their obvious lack of appeal analytically, piecewise-smooth differential equations have found application in mechanics, biological modelling, computer science, control, and electrical engineering. Under generic conditions, the bifurcations that such models can undergo, so-called *discontinuity induced bifurcations*, are known to fit within a

reasonably small number of normal forms, prominent amongst which are the sliding bifurcations in non-differentiable flows [5], and the border collisions in non-differentiable maps [3, 18]. Except in low dimensional cases there is still no obvious classification of the dynamics near these bifurcations and there is a risk, in consequence, that the literature becomes filled with ever more complicated examples.

In this paper we show that there is a link between two of these normal forms, in the sense that one of them arises as an induced map in the analysis of the other. We hope that this is the beginning of a more coherent description of the inter-relatedness of different models, and in particular, that this will aid in the understanding of bifurcations in high dimensional nonsmooth systems. We also discuss the possible attractors that can occur in these models. Our results suggest that the bifurcation theory of piecewise-smooth systems suffers from the curse of dimensionality [1], in that the description of a bifurcation on $\mathbb{R}^n$ depends crucially on n. This is in marked contrast to the case of local bifurcation theory for smooth systems, where the centre manifold theorem (see e.g. [14]) ensures that only the eigenvectors and eigenvalues, together with some genericity and transversality conditions, determine any invariant sets that are created at the bifurcation.

Border collision bifurcations occur when phase space is divided into two regions by a switching surface, and differentiable discrete time dynamics is defined separately in each region, by maps that are continuous across the switching surface but whose Jacobians may be discontinuous. If a fixed point in one region varies with changing parameters so that at some critical parameter it intersects the switching surface transversely, then a border collision is said to occur. Provided the switching surface is not singular at the point where the fixed point intersects it, the local dynamics near such bifurcations can be described by a continuous piecewise linear map in terms of coordinates $z = (z_1, \ldots, z_n)^T \in \mathbb{R}^n$ chosen so that the switching surface is (locally) $z_1 = 0$, so

$$z' = \begin{cases} A_L z + m & \text{if } z_1 < 0 \\ A_R z + m & \text{if } z_1 > 0 \end{cases} \tag{1}$$

where the parameter m can be written in terms of a real parameter ν as

$$m = (\nu, 0, 0, \ldots, 0)^T$$

and A_L and A_R are constant $n \times n$ matrices. Continuity across $z_1 = 0$ implies that for any $z_0 = (0, z_2, \ldots, z_n)^T$

$$A_L z_0 = A_R z_0. \tag{2}$$

The border collision normal form, derived by Nusse and Yorke [18] in two-dimensions, and by di Bernardo [3, 6] in higher dimensions, is obtained by making a particular choice for the coordinate system so that in two dimensions

$$A_L = \begin{pmatrix} T_L & 1 \\ -D_L & 0 \end{pmatrix}, \qquad A_R = \begin{pmatrix} T_R & 1 \\ -D_R & 0 \end{pmatrix}, \tag{3}$$

whilst in higher dimensions both A_L and A_R can be put into observer canonical form [3]

$$
A_j = \begin{pmatrix}
\omega_{j1} & 1 & 0 & \ldots & 0 & 0 \\
\omega_{j2} & 0 & 1 & \ldots & 0 & 0 \\
\omega_{j3} & 0 & 0 & \ldots & 0 & 0 \\
\vdots & \vdots & \vdots & \ddots & \vdots & \vdots \\
\omega_{j(n-1)} & 0 & 0 & \ldots & 0 & 1 \\
\omega_{jn} & 0 & 0 & \ldots & 0 & 0
\end{pmatrix}, \tag{4}
$$

with j taking the two labels L and R (so $w_{j1} = T_j$ and $w_{j2} = -D_j$ in two dimensions). The transformations that lead to the observer canonical form are possible for generic maps of the general form (1), but, crucially for the analysis in our final section, not every map of the form (1). The genericity condition is essentially the non-singularity of the matrices A_L and A_R together with an associated matrix having full rank (see [18, 3] for details). We will refer to the general continuous piecewise smooth maps (1) as border collision maps, whilst if they can be transformed to observer canonical form the transformed maps will be called border collision normal forms.

These have been studied in their own right before their derivation as normal forms in piecewise-smooth systems, see e.g. [17]. Note that by a linear rescaling of the variables z_j the parameter ν may be chosen without loss of generality to be either 0 or 1.

The *grazing-sliding* normal form describes a bifurcation of piecewise-smooth flows (*Filippov* systems). As in the border collision normal form, phase space is divided into two regions by a switching surface, and in this case, differentiable continuous time dynamics is defined separately in each region by ordinary differential equations. If a periodic orbit in one region becomes tangent to the switching surface at an isolated point for some critical value of a parameter, and the vector field defining the dynamics in the other region points towards the switching surface at this point, a grazing-sliding bifurcation is said to occur. The term *sliding* refers to nearby solutions that typically include segments of sliding along the switching surface. In two dimensions these bifurcations can be described relatively easily [5, 16], but in three dimensions the situation is already considerably more complicated [11, 12]. Here we consider the case of grazing-sliding bifurcations in $\mathbb{R}^n$, $n \geq 4$.

Our main results are the following. Firstly, the $(n-2)$-dimensional border collision normal form arises in the study of n-dimensional grazing-sliding bifurcations, thus providing an example of how different areas of piecewise smooth bifurcation analysis are linked. Second we show that the n-dimensional border collision normal form can have invariant sets that are themselves of topological dimension n and on which periodic orbits are dense (and other properties typical of chaotic behaviour also hold). We use this to show that for any $k \in \{0, 1, \ldots, n\}$ there exist general border collision maps on $\mathbb{R}^n$ with invariant sets which have topological dimension k. This shows that the topological nature of the invariant sets of border collision bifurcations can have structure which depends crucially on the dimension of the phase space. Since completing this work

it has also been shown that the n-dimensional border collision normal form can have attractors with topological dimension n for many parameter values (see [10], adapting the results of [19, 7, 8]). So the special cases described here, which are not attractors in the same sense that the interval $[0, 1]$ of the logistic map $f(x) = 4x(1 - x)$ is not an attractor having no larger open set whose orbits tend to it, are examples of a much more general phenomenon. The examples described here have the advantage that properties such as dense periodic orbits and transitivity can be verified directly.

In the next section we describe the conditions for a grazing-sliding bifurcation to occur in piecewise-smooth systems in $\mathbb{R}^n$ (see e.g. [5]), and show how to reduce this to an $(n - 2)$-dimensional return mapping, following the procedure adopted in [11] for $n = 3$. In section 3 we treat the four dimensional case, showing the formal reduction to the border collision normal form (1), under certain conditions. In section 4 we give specific examples that show these conditions can be satisfied. Sections 5 and 6 generalize the previous two sections to higher dimensions. In section 7 we describe how the n-dimensional border collision normal can have invariant sets of topological dimension n and deduce as a corollary that border collision maps can have invariant sets with any given non-negative integer dimension less than or equal to n.

2. Grazing-sliding in $\mathbb{R}^n$

The piecewise-smooth systems we consider are defined by two sets of smooth differential equations whose regions of definition are separated by a smooth manifold Σ, the switching surface. We write these as

$$(\dot{x}, \dot{y}, \dot{\underline{z}}) = \begin{cases} f_+(x, y, \underline{z}; \mu) & \text{if} \quad h(x, y, \underline{z}; \mu) > 0, \\ f_-(x, y, \underline{z}; \mu) & \text{if} \quad h(x, y, \underline{z}; \mu) < 0, \end{cases} \tag{5}$$

where $f_\pm$ are smooth functions of the variables $(x, y, \underline{z})$ and a parameter μ. It is useful to think of f_+ and f_- each being defined on the whole of $\mathbb{R}^n$. We have separated out $x, y \in \mathbb{R}$, and $\underline{z} = (z_1, z_2, ..., z_{n-2}) \in \mathbb{R}^{n-2}$, so that x and y can be chosen as follows (see Figure 2). Without loss of generality, y can be chosen so that the switching surface is given by

$$\Sigma = \{(x, y, \underline{z}) \in \mathbb{R}^n \mid y = 0\}.$$

Then x is chosen such that the surface

$$\Pi = \{(x, y, \underline{z}) \in \mathbb{R}^n \mid x = 0\}$$

is the locus of points where

$$f_+^{(y)}(x, y, \underline{z}; \mu) = 0, \tag{6}$$

using the notation $f^{(y)}$ to denote the y component of a vector f (and similarly for $f^{(x)}$, and so on). We assume that

$$f_+^{(x)}(0, 0, \underline{0}; 0) > 0 \quad \text{and} \quad \frac{\partial f_+^{(y)}}{\partial x}(0, 0, \underline{0}; 0) > 0, \tag{7}$$

so the surface Π is the locus of tangential intersections of the vector field f_+ with $y = 0$, where f_+ curves quadratically away from the switching surface. Since $f_+^{(x)}(0, 0, \underline{0}; 0) \neq 0$, Π is also transverse to the flow of f_+ at the origin. Therefore Π can be used as a local section to define a Poincaré map for the flow in the vector field f_+. Hence we define a return map

$$P_\Pi : \Pi \times \mathbb{R} \mapsto \Pi,$$

assuming f_+ is defined over the whole of $\mathbb{R}^n$, neglecting for the moment the switch at $y = 0$.

A grazing bifurcation is said to occur when a periodic orbit is tangent to the switching surface Σ at an isolated point for a critical value of a parameter. We now assume that a grazing bifurcation takes place at $(x, y, \underline{z}) = (0, 0, \underline{0})$ when $\mu = 0$, and that the grazing periodic orbit is a fixed point of the map P_Π. We also assume a parametric transversality condition, namely that the fixed point of P_Π moves through $y = 0$ with non-zero velocity as μ passes through zero; more detail is given the Appendix (see also [4, 5]).
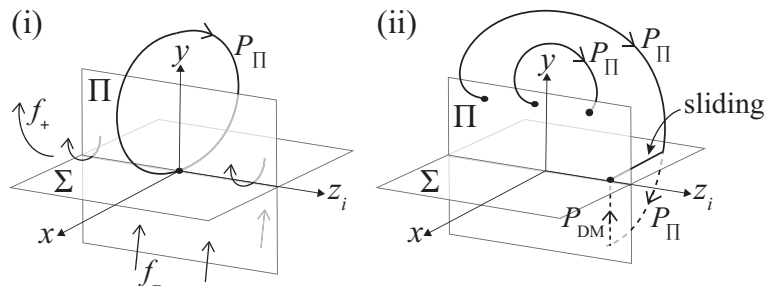

Figure 1. (i) The grazing periodic orbit, in coordinates $(x, y, \underline{z}) = (x, y, (z_1, z_2, ...))$, with vector fields f_+ and f_- either side of the switching surface Σ. (ii) The return map P_Π on Π is valid for $y > 0$, and in $y < 0$ a correction P_{DM} accounts for the occurence of sliding.

Whilst the flow in $y > 0$ defines the *grazing* part of a grazing-sliding bifurcation, the *sliding* part is furnished by also considering the properties of f_-. We assume $f_-^{(y)}(0, 0, \underline{0}; 0) > 0$, so that f_- points locally towards Σ. Considering also the sign of $f_+^{(y)}$, by (6) we have $f_+^{(y)}(x, 0, \underline{z}; \mu) < 0$ in $x < 0$, so that there is a region of values of x on Σ on which both vector fields $f_\pm$ point towards Σ. This confines the flow of (5) to a sliding component on Σ, which is generally modelled by taking the linear combination of f_+ and f_- that lies tangent to Σ. This sliding motion terminates on the surface $x = 0$ (in $y = 0$) where $f_+^{(y)}$ changes sign, so that when it reaches Π the flow lifts off from Σ back into $y > 0$.

Details of how to define sliding solutions are given in any standard text (e.g. [6, 9], see also Appendix A). The important point is that when sliding is taken into account the model of the dynamics near the grazing orbit can be reduced to an $(n - 2)$-dimensional return map on the surface $\Pi \cap \Sigma$, i.e. $x = y = 0$. The return map $P_\Pi : \Pi \mapsto \Pi$ neglects the switch at $y = 0$, in particular the sliding motion that brings the flow to $x = 0$. This

is easily corrected by composing P_Π with a local reset

$$P_{DM} : \Pi \times \mathbb{R} \to \Pi \cap \Sigma,$$

called a Poincaré Discontinuity Map [5]. The parameter dependence of P_{DM} lies in the nonlinear terms, so the linearization of the P_{DM} used below is independent of the parameter. The composition $P_{DM} \circ P_\Pi^k$, for appropriate k (where the y-component of P_Π^k lies in $y < 0$), gives a family of return maps parametrized by μ on the set $\Pi \cap \Sigma$, which is the intersection of the return plane Π with the sliding surface on Σ, and also the locus of solutions that lift off into $y > 0$ from the sliding surface. This map is piecewise continuous (discontinuities corresponding to orbits undergoing grazing). Essentially P_Π is applied to a point $(0, 0, \underline{z}) \in \Pi \cap \Sigma$, and iterated until the y-component of $P_\Pi^k(0, 0, \underline{z}; \mu)$ becomes negative for the first time. Then P_{DM} is applied to bring the solution back to where it would have intersected $\Pi \cap \Sigma$ had the sliding component been taken into account.

This informal account is enough to make the following sections comprehensible if the reader is prepared to take the stated linearizations of P_Π and P_{DM} on trust. The omitted details are given in the Appendix, together with a discussion about the choice of coordinates. In particular, regarding the Poincaré map P_Π, we are implicitly assuming here that, except for the point $(x, y, \underline{z}) = (0, 0, \underline{0})$, the grazing periodic orbit lies only in $y > 0$. This can be relaxed to allow entry to $y \leq 0$ far away from $(x, y, \underline{z}) = (0, 0, \underline{0})$, provided certain transversality conditions hold, and we remark on this in Section 8. A peculiarity of grazing-sliding bifurcations is that the derivative of P_{DM} is nonzero at $y = 0$, in contrast to the maps associated with other codimension one sliding bifurcations [5, 6], implying that they are not affected by much of the interesting behaviour that we find here for grazing-sliding. In the next section we give explicit forms for P_Π and P_{DM} in four dimensions, followed by examples, before giving general n-dimensional forms in Section 5.

3. Grazing-sliding bifurcations in four dimensions

Consider a system of four variables $(x, y, z_1, z_2) \in \mathbb{R}^4$ as described in the previous section, so that they vary in time forming a periodic orbit that grazes from $y > 0$ when $\mu = 0$. The linearization of the return map P_Π close to the periodic orbit can be described in observer canonical form (see Appendix A) as

$$\begin{pmatrix} y' \\ z_1' \\ z_2' \end{pmatrix} = \begin{pmatrix} a & 1 & 0 \\ b & 0 & 1 \\ c & 0 & 0 \end{pmatrix} \begin{pmatrix} y \\ z_1 \\ z_2 \end{pmatrix} + \mu \begin{pmatrix} 1 \\ 0 \\ 0 \end{pmatrix}. \tag{8}$$

After each iteration, if $y' > 0$ then the flow misses the switching surface and the map is iterated again. If $y' < 0$ then P_Π neglects the fact that the flow has reached the switching surface a little before the intersection with $x = 0$. To correct this, the value of y' needs to be adjusted using the Poincaré Discontinuity Map [4, 5] to take the solution back

to the sliding surface $y = 0$, and then evolve it along the switching surface to the next point at which the solution can leave the sliding surface, viz. $x = y = 0$. Expanding solutions as power series in the (small) time taken to make this adjustment leads to the general form for the linearization of P_{DM}

$$\begin{pmatrix} y'' \\ z_1'' \\ z_2'' \end{pmatrix} = \begin{pmatrix} 0 & 0 & 0 \\ \alpha & 1 & 0 \\ \beta & 0 & 1 \end{pmatrix} \begin{pmatrix} y' \\ z_1' \\ z_2' \end{pmatrix}. \tag{9}$$

If a solution starts on the surface Π with $y = 0$ (the 'lift-off' surface $\Pi \cap \Sigma$), the return map (8) brings the trajectory from $(0, z_1, z_2)$ back to Π at

$$(z_1 + \mu, z_2, 0).$$

If $z_1 + \mu < 0$, the linearized Poincaré discontinuity mapping (9) brings the solution back to $x = 0$ with

$$(z_1'', z_2'') = (\alpha(z_1 + \mu) + z_2, \beta(z_1 + \mu)). \tag{10}$$

If $z_1 + \mu > 0$ then the modelled trajectory lies entirely in $y > 0$ during this part of its motion and the return map (8) is applied again, giving

$$(a(z_1 + \mu) + z_2 + \mu, b(z_1 + \mu) + z_2, c(z_1 + \mu)).$$

Now, if $a(z_1 + \mu) + z_2 + \mu > 0$ the solution goes round in $y > 0$ again, whilst if $a(z_1 + \mu) + z_2 + \mu < 0$ (9) is applied to find the next intersection with $y = 0$ (i.e. Σ) on the surface $x = 0$ (i.e. Π), which is

$$(z_1'', z_2'') = (\alpha a + b, \beta a + c)(z_1 + \mu) + (\alpha, \beta)(z_2 + \mu) + (z_2, 0). \tag{11}$$

Thus, writing $Z_1 = z_1 + \mu$ and $Z_2 = z_2 + \mu$, the dynamics of solutions that go once or twice round the cycle in $y > 0$ before having a sliding segment can be described by the maps

$$(z_1'', z_2'') = \begin{cases} (\alpha, \beta)Z_1 + (Z_2 - \mu, 0) & \text{if } Z_1 < 0, \\ (\alpha, \beta)(aZ_1 + Z_2) + (b, c)Z_1 & \text{if } Z_1 > 0 \text{ and } aZ_1 + Z_2 < 0, \\ \text{undefined} & \text{otherwise,} \end{cases} \tag{12}$$

where the term 'undefined' indicates that further analysis is required to determine the next intersection after a sliding segment. Writing these evolution equations using coordinates Z_1 and Z_2 throughout and replacing the iteration double primes with single primes, we obtain

$$(Z_1', Z_2') = F(Z_1, Z_2; \mu) \tag{13}$$

where $F : \mathbb{R}^2 \times \mathbb{R} \to \mathbb{R}^2$ is defined by

$$\begin{cases} (\alpha Z_1 + Z_2, \beta Z_1 + \mu) & \text{if } Z_1 \leq 0, \\ (\alpha a + b, \beta a + c)Z_1 \\ \quad + (\alpha, \beta)Z_2 + \mu(1, 1) & \text{if } Z_1 > 0 \text{ and } aZ_1 + Z_2 < 0, \\ \text{undefined} & \text{otherwise.} \end{cases} \tag{14}$$

It will be useful to refer to the two maps as

$$F_1(Z_1, Z_2; \mu) = (\alpha Z_1 + Z_2, \beta Z_1 + \mu) \tag{15}$$

and

$$F_2(Z_1, Z_2; \mu) = ((\alpha a + b)Z_1 + \alpha Z_2 + \mu, (\beta a + c)Z_1 + \beta Z_2 + \mu), \tag{16}$$

so

$$F(Z_1, Z_2; \mu) = \begin{cases} F_1(Z_1, Z_2; \mu) & \text{if } Z_1 \leq 0, \\ F_2(Z_1, Z_2; \mu) & \text{if } Z_1 \geq 0. \end{cases} \tag{17}$$

The ambiguity allowed here if $Z_1 = 0$ will be resolved shortly.

There are now two ways an orbit may go twice around a cycle before sliding: it may slide only after the second cycle and be given by F_2, or it may slide after each cycle and be given by F_1 applied twice, see Figure 2. To describe this we define a map G as follows.
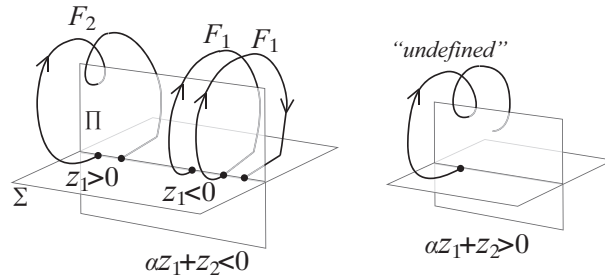

Figure 2. The return maps F_2 and F_1^2 on the grazing set $\Sigma \cap \Pi$, with two and one sliding segments per orbit respectively. Also shown (right) is the case where a second return map on $\Sigma \cap \Pi$ cannot be defined, because an orbit does not slide after two cycles.

Let

$$\begin{aligned} D_1 &= \{(Z_1, Z_2) \mid Z_1 \leq 0, \quad \alpha Z_1 + Z_2 < 0\}, \\ D_2 &= \{(Z_1, Z_2) \mid Z_1 \geq 0, \quad a Z_1 + Z_2 < 0\}, \end{aligned} \tag{18}$$

and

$$D = D_1 \cup D_2. \tag{19}$$

Lemma 1 *The map* $G : D \times \mathbb{R} \to \mathbb{R}^2$ *defined by*

$$G(Z_1, Z_2; \mu) = \begin{cases} F_1^2(Z_1, Z_2; \mu) & \text{if } (Z_1, Z_2) \in D_1 \\ F_2(Z_1, Z_2; \mu) & \text{if } (Z_1, Z_2) \in D_2 \end{cases} \tag{20}$$

is continuous, and if there exists $N > 0$ *such that* $G^k(Z_1, Z_2; \mu) \in D$ *for* $k = 0, \ldots, N$, *then*

$$G^k(Z_1, Z_2; \mu) = F^m(Z_1, Z_2; \mu) \tag{21}$$

where $m = k + j_k$ *and* j_k *is the number of times the map in* D_1 *is used in the iteration of* G.

Proof: If $(Z_1, Z_2) \in D_1$ then $F(Z_1, Z_2; \mu) = F_1(Z_1, Z_2; \mu) = (\alpha Z_1 + Z_2, \beta Z_1 + \mu)$ and so $F_1(Z_1, Z_2; \mu) \in \{Z_1 \leq 0\}$ by the definition of D_1 and $F^2(Z_1, Z_2; \mu) = F(F_1(Z_1, Z_2; \mu); \mu) = F_1^2(Z_1, Z_2; \mu)$ and by direct calculation this is

$$((\alpha^2 + \beta)Z_1 + \alpha Z_2 + \mu, \alpha\beta Y + \beta Z_2 + \mu), \quad (Z_1, Z_2) \in D_1. \tag{22}$$

In particular, F_1^2 is well defined for $(Z_1, Z_2) \in D_1$. Since F_1 and F_2 are continuous, G is continuous provided it is continuous on $Z_1 = 0$, and by (22)

$$F_1^2(0, Z_1; \mu) = (\alpha Z_2 + \mu, \beta Z_2 + \mu) = F_2(0, Z_2; \mu)$$

where the second equality follows from (16). Hence G is continuous and the equality (21) follows as $G = F^2$ on D_1 and $G = F$ on D_2.

$\square$

If (Z_1, Z_2) lies outside D, that is if $\alpha Z_1 + Z_2 > 0$ by (18), then the orbit will not slide at the end of two cycles and a third application of the return map on Π will be required; we are not concerned with such orbits here.

Note that if $G^k(Z_1, Z_2; \mu) = (0, \zeta)$ for some ζ then there is a choice about whether to apply the map defined in D_1 or the map in D_2. We assume in the statement of the lemma that the same choice is made in the evaluation of both G and F. The continuity of G implies that this makes no difference to the eventual orbit.

The importance of this lemma is that it implies that if G has an attractor in D then there is a corresponding attractor of F in $\{Z_1 \leq 0\} \cup D_2$, and the action of G restricted to this set is linearly conjugate to the attractor of a border collision normal form with appropriately chosen parameters. These results are formalized in Corollaries 2 and 3 below.

Corollary 2 *If $G|_D$ has an attracting set then F has an attracting set in $\{Z_1 \leq 0\} \cup D_2$.*

This is obvious from Lemma 1.

Corollary 3 *If $G|_D$ has an attracting set then $G|_D$ is linearly conjugate to the border collision normal form restricted to some appropriate domain $E \subseteq \mathbb{R}^2$ containing at least one attractor. The parameters of the border collision normal form can be chosen so that*

$$A_L = \begin{pmatrix} \alpha^2 + 2\beta & 1 \\ -\beta^2 & 0 \end{pmatrix} \quad A_R = \begin{pmatrix} \alpha a + b + \beta & 1 \\ -(\beta b - \alpha c) & 0 \end{pmatrix} \tag{23}$$

with $sign(\nu) = sign(\mu)$, where ν corresponds to the parameter of the border collision normal form as in (1).

Proof: The determinant and trace of the two linear maps (16) and (22) are easy to calculate and the coordinate changes are essentially those used by Nusse and Yorke to obtain the normal form [18]. (The first column of the border collision normal form is the trace and minus the determinant of the map.) The only complication is the sign of μ (by a linear rescaling it is only the sign of μ that determines the dynamics), and this follows from the observation that $G(0, 0; \mu) = (\mu, \mu)$ which is in D_2 if $\mu > 0$ and $Z_1 \leq 0$ if $\mu < 0$. The corresponding point for the border collision normal form is also $(0, 0)$, hence the result.
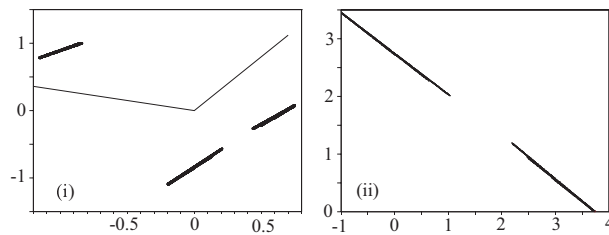
$\square$

Figure 3. The thin attractor. (i) The attractor of grazing sliding map with parameters (24) also showing the boundary of D. (ii) The attractor of the border collision normal form with parameters (25).

4. Two examples

The results of the previous section establish a formal connection between the attractors of the linearized grazing-sliding normal form F, an induced map G and the border collision normal form. However, the attractor of G must lie in the region D of equation (19) for the results to be applicable, and we have not established conditions for this to be the case. In particular it might never be the case!

In this section we show numerically that there are attractors with the desired properties, and hence that the there is content in the results described above. The two examples are chosen to illustrate different geometries of the attractor – in the first the attractor is nearly a union of curves (though it actually appears to have a fractal structure) and in the second the attractor occupies a much larger region of phase space.

The first example is illustrated in Figure 3. This has parameters

$$
\begin{aligned}
&a = -1.6, \quad b = -1.15, \quad c = -1.15, \\
&\alpha = 0.3, \quad \beta = 1.1, \quad \mu = 1;
\end{aligned}
\tag{24}
$$

for F, which translate to

$$
\begin{aligned}
&T_L = 2.29, \quad D_L = 1.21, \quad T_R = -0.53, \\
&D_R = -0.92, \quad \nu = 1;
\end{aligned}
\tag{25}
$$

for the border collision normal form, with T_L the trace of A_L, D_L the determinant of A_L and similarly for A_R. The attractor of F is shown in Figure 3(i) (and the attractor for G is the part shown in the region D), whilst the attractor of the corresponding border collision normal form is shown in Figure 3(ii).

The second example is illustrated in Figure 4 with the same layout and

$$
\begin{aligned}
&a = -1.8, \quad b = -1.4, \quad c = -1.4, \\
&\alpha = 0.4, \quad \beta = 1.2, \quad \mu = 1;
\end{aligned}
\tag{26}
$$

for F, which translate to

$$
\begin{aligned}
&T_L = 2.56, \quad D_L = 1.44, \quad T_R = -0.92, \\
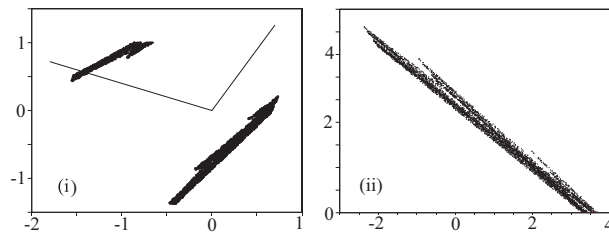&D_R = -1.12, \quad \nu = 1;
\end{aligned}
\tag{27}
$$

Figure 4. The thick attractor, as Figure 3 but using parameters (26) and (27).

5. The general case

The results of section 3 used a special choice for the return map of the grazing orbit and restricted to only four dimensions, leading to a two-dimensional model. This was done so that the geometry could be easily appreciated and examples found. In this section we consider the general case, both in terms of the return map and the dimension, and show that results analogous to those of section 3 hold again, with the border collision normal form of Nusse and Yorke replaced by the $(n-2)-$dimensional generalization of di Bernardo [3, 6].

The following two Lemmas express these in a convenient form, without loss of generality.

Lemma 4 *The return map on* Π *in* $x > 0$ *can be generally written near the periodic orbit as*

$$\begin{pmatrix} y' \\ \underline{z}' \end{pmatrix} = \begin{pmatrix} a & \underline{u}^T \\ \underline{b} & \underline{\underline{U}} \end{pmatrix} \begin{pmatrix} y \\ \underline{z} \end{pmatrix} + \mu \begin{pmatrix} 1 \\ \underline{0} \end{pmatrix} \tag{28}$$

where the constant coefficients include a column vector of zeros $\underline{0}$*, the scalar* a*, and* $(n-2)$ *dimensional vectors* $\underline{b}$*,* $\underline{u}$*, and square matrix* $\underline{\underline{U}}$*, given by*

$$\underline{b} = \begin{pmatrix} b_1 \\ b_2 \\ \vdots \\ b_{n-2} \end{pmatrix}, \quad \underline{u} = \begin{pmatrix} 1 \\ 0 \\ \vdots \\ 0 \end{pmatrix}, \quad \underline{\underline{U}} = \begin{pmatrix} 0 & 1 & 0 & 0 & \dots \\ 0 & 0 & 1 & 0 & \dots \\ \vdots & \vdots & \vdots & \ddots & \dots \\ 0 & 0 & 0 & \dots & 0 \end{pmatrix}. \tag{29}$$

Lemma 5 *The discontinuity map to* Π *can be generally written near the periodic orbit as*

$$\begin{pmatrix} y'' \\ \underline{z}'' \end{pmatrix} = \begin{pmatrix} 0 & \underline{0}^T \\ \underline{\alpha} & \underline{\underline{1}} \end{pmatrix} \begin{pmatrix} y' \\ \underline{z}' \end{pmatrix} \tag{30}$$

where $\underline{\underline{1}}$ *is the* $(n-2)\times(n-2)$ *identity matrix and* $\underline{\alpha}$ *is the column vector with components* $(\alpha_1, \alpha_2, ..., \alpha_{n-1})$*.*

The proofs of these lemmas is given in Appendix A. Let us briefly review how they are applied to obtain a general orbit returning to $x = y = 0$. Applying P_Π to a point $(0, \underline{z})$ on $\Pi \cap \Sigma$ gives a return coordinate $(y', \underline{z}') = P_\Pi(0, \underline{z})$ on Π, which neglects the

existence of the discontinuity. This omission is corrected by applying the discontinuity mapping P_{DM}. If $y' < 0$ then P_{DM} maps $(y', \underline{z}')$ to a point $(0, \underline{z}'')$ on $\Pi \cap \Sigma$. If $y' > 0$ then the orbit has missed the switching surface and we apply P_{Π} again, and do so repeatedly until the image coordinate $y''''^{\cdots}$ under P_{Π} becomes negative, which is only then corrected by applying P_{DM} to give the return to $\Pi \cap \Sigma$. We are interested only in orbits that eventually slide, and hence return to the set $x = y = 0$.

A point $(0, 0, \underline{z})$ that first returns to some $(0, 0, \underline{z}'')$ on its mth return to Π is described by a map from $\Pi \cap \Sigma \times \mathbb{R}$ to $\Pi \cap \Sigma$, given by

$$\begin{pmatrix} 0 \\ \underline{z}'' \end{pmatrix} = P_{DM} \circ P_{\Pi}^m (0, \underline{z}; \mu)$$

$$= C\Lambda^m \begin{pmatrix} 0 \\ \underline{z} \end{pmatrix} + \mu C (\Lambda^{m-1} + \Lambda^{m-2} + ... + I) \begin{pmatrix} 1 \\ \underline{0} \end{pmatrix} \tag{31}$$

where C and Λ are the $(n-1$-dimensional square matrices defined in (28) and (30) respectively. Taking only the $\underline{z}$ part gives a map on the grazing set $x = y = 0$, namely

$$\underline{z}'' = F_m(\underline{z}; \mu)$$

$$= (\underline{\alpha}, \ \underline{\underline{1}}) \cdot \left[\Lambda^m \begin{pmatrix} 0 \\ \underline{z} \end{pmatrix} + \mu (\Lambda^{m-1} + \Lambda^{m-2} + ... + I) \begin{pmatrix} 1 \\ \underline{0} \end{pmatrix} \right]. \tag{32}$$

The domain of F_m is

$$\{ \underline{z} \in \mathbb{R}^{n-2} : \ [P_{\Pi}^m(0, \underline{z}; \mu)]^{(y)} \leq 0 \leq [P_{\Pi}^i(0, \underline{z}; \mu)]^{(y)}, \ \forall i \in [1, m-1] \}.$$

At first sight there may appear to be a contradiction: how can a continuous flow give rise to a discontinuous return map? The explanation is shown in Figure 5: the discontinuities are caused by grazing, in whose vicinity the flow can hit the switching surface, or miss it and take some finite time before returning again. Continuity is restored by considering the maps describing grazing orbits in the following way. Consider the orbit of a point $\underline{z}$ that grazes upon its κth return to Π, and subsequently slides during its mth to Π such that $0 < \kappa < m$. The mth iterate is given equivalently by both

$$\underline{z} \mapsto F_m(\underline{z}; \mu) \qquad \text{and} \qquad \underline{z} \mapsto F_{m-\kappa} \circ F_{\kappa}(\underline{z}; \mu). \tag{33}$$

This condition is illustrated in Figure 5. More precisely, such an orbit satisfies the conditions $[P_{\Pi} \circ P_{\kappa-1}(0, \underline{z}; \mu)]^{(y)} = 0$ (grazing on the κth iteration), and $[P_{\Pi} \circ P_{m-1}(0, \underline{z}; \mu)]^{(y)} < 0 < [P_{\Pi} \circ P_{j-1}(0, \underline{z}; \mu)]^{(y)}$ for $j \in [1, \kappa - 1] \cup [\kappa + 1, m - 1]$ (sliding only on the mth iteration).

Henceforth let us restrict attention to orbits that wind around in $y \geq 0$ twice before returning to $x = y = 0$, given by F_1^2 or F_2, the difference being that the discontinuity mapping is applied in both windings of F_1^2, but only the second winding of F_2.

We now return to the results of Lemmas 4 and 5 and, as in section 3, define the shifted coordinates $Z_i = z_i + \mu$ for all $i = 1, 2, ..., n-2$. The map G defined in Lemma 1, for orbits that wind around twice in $y \geq 0$ before returning to $x = y = 0$, can be
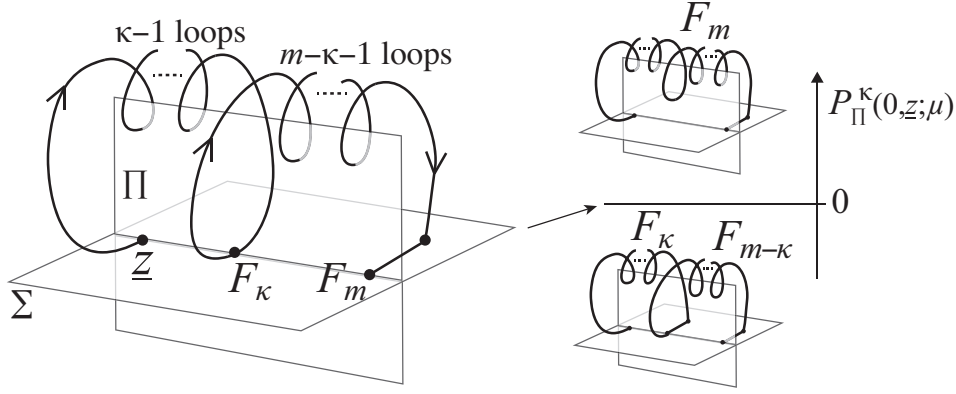
Figure 5. The continuity condition between F_m and $F_{m-\kappa} \circ F_\kappa$.

calculated in n-dimensions directly from Lemmas 4 and 5. It consists of the Poincaré map composed with the discontinuity map, given by

$$
\begin{aligned}
F_1(\underline{Z}; \mu) = \quad & (\ \alpha_1 Z_1 + Z_2, \ \alpha_2 Z_1 + Z_3 + \mu, \ \alpha_3 Z_1 + Z_4, \ \dots, \\
& \alpha_{n-3} Z_1 + Z_{n-2}, \ \alpha_{n-2} Z_1 + \mu \ ),
\end{aligned}
\tag{34}
$$

if $Z_1 < 0$, and of two applications of the Poincaré map composed with the discontinuity map, which gives

$$
\begin{aligned}
F_2(\underline{Z}; \mu) = \quad & (\ (\alpha_1 a + b_1) Z_1 + \alpha_1 Z_2 + Z_3, \\
& (\alpha_2 a + b_2) Z_1 + \alpha_2 Z_2 + Z_4, \\
& (\alpha_3 a + b_3) Z_1 + \alpha_3 Z_2 + Z_5, \\
& \dots, \\
& (\alpha_{n-4} a + b_{n-4}) Z_1 + \alpha_{n-4} Z_2 + Z_{n-2}, \\
& (\alpha_{n-3} a + b_{n-3}) Z_1 + \alpha_{n-3} Z_2 + \mu, \\
& (\alpha_{n-2} a + b_{n-2}) Z_1 + \alpha_{n-2} Z_2 + \mu \ )
\end{aligned}
\tag{35}
$$

if $Z_1 > 0$ and $a Z_1 + Z_2 < 0$.

Let $\underline{Z} = (Z_1, Z_2, \dots, Z_{n-2})$. Then the regions D_1 and D_2 of (18) on (Z_1, Z_2) become (with the obvious abuse of notation)

$$
\begin{aligned}
D_1 &= \{ \underline{Z} \in \mathbb{R}^{n-2} \mid Z_1 \leq 0, \ \alpha Z_1 + Z_2 < 0 \}, \\
D_2 &= \{ \underline{Z} \in \mathbb{R}^{n-2} \mid Z_1 \geq 0, \ a Z_1 + Z_2 < 0 \},
\end{aligned}
\tag{36}
$$

and if $D = D_1 \cup D_2$ then the general form of Lemma 1 is:

Lemma 6 *The map $G : D \times \mathbb{R} \to \mathbb{R}^{n-2}$ defined by*

$$
G(\underline{Z}; \mu) = \begin{cases} F_1^2(\underline{Z}; \mu) & \text{if } \underline{Z} \in D_1 \\ F_2(\underline{Z}; \mu) & \text{if } \underline{Z} \in D_2 \end{cases}
\tag{37}
$$

is continuous and if there exists $N > 0$ such that $G^k(\underline{Z}; \mu) \in D$ for $k = 0, \dots, N$, then

$$
G^k(\underline{Z}; \mu) = F^m(\underline{Z}; \mu)
\tag{38}
$$

where $m = k + j_k$ and j_k is the number of times the map in D_1 is used in the iteration of G up to the kth iterate.
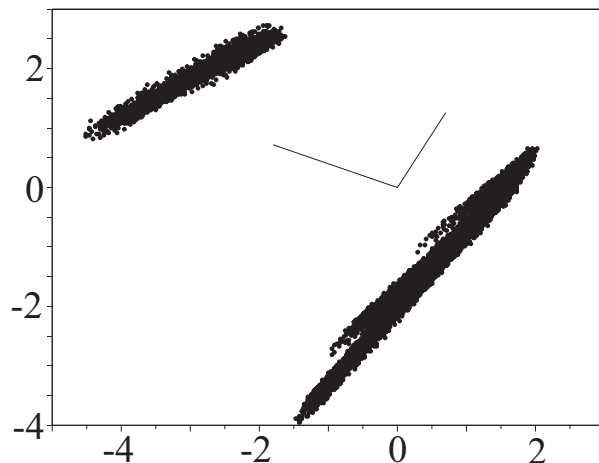
Figure 6. The attractor in $\mathbb{R}^{20}$, projected onto the first two coordinates. See text for parameter values, (39).

Corollary 7 *If $G|_D$ has an attracting set then $G|_D$ is linearly conjugate to the border collision normal form restricted to some appropriate domain $E \subseteq \mathbb{R}^2$ containing at least one attractor.*

6. High dimensional examples

As in the four dimensional case, the analysis of the previous section shows a correspondence between solutions of the grazing-sliding normal form and the border collision normal form provided that some conditions hold; in particular the attractor of the appropriate iterates of the grazing-sliding normal form must lie in the region $D_1 \cup D_2$. As before, analytical conditions for the existence of such an attractor have not been established. The aim of this section is to provide two examples, one in 20 dimensions and one in 100 dimensions, to show that there are parameters at which these conditions are satisfied. Both examples are extensions of the second example of section 4.

The first, in $\mathbb{R}^{20}$ (so applicable to flows in $\mathbb{R}^{22}$), takes the system defined by (34) and (35) with

$$
\begin{aligned}
&a = -1.8, \quad b_1 = -1.4, \quad b_2 = -1.4, \\
&b_r = 0.05, \ r = 3, \ldots, 20, \\
&\alpha_1 = 0.4, \quad \alpha_2 = 1.2, \\
&\alpha_r = -0.05, \ r = 3, \ldots, 20, \quad \mu = 1.
\end{aligned}
\tag{39}
$$

Figure 6 shows the projection onto the (Z_1, Z_2) plane of the attractor, together with the half-lines $aZ_1 + Z_2 = 0$ (in $Z_1 < 0$) and $\alpha_1 Z_1 + Z_2 = 0$ (in $Z_1 > 0$). As in the low dimensional example this shows that the attractor is in two parts, one of which is below these lines and it is here that the induced map can be defined, the other is the image of the subset of this part of the attractor that lies in $Z_1 < 0$, and this is also in $Z_1 < 0$ as
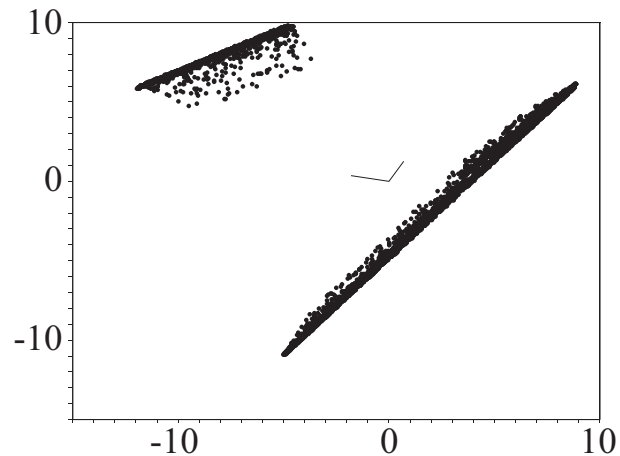
Figure 7. The attractor in $\mathbb{R}^{100}$, projected onto the first two coordinates. See text for parameter values, (40).

it must be for F_1^2 to be defined for the induced map. 10000 iterates are shown after an initial transient of 501 iterates from the initial condition

$$z_1 = -0.001, \quad z_2 = -0.005,$$
$$z_r = 0, \ r = 3, \dots, 20.$$

We have verified that the picture remains effectively unchanged after 100000 iterates.

The second attractor, shown in Figure 7 is in $\mathbb{R}^{100}$ (so applicable to flows in $\mathbb{R}^{102}$), which is large enough to support a conjecture that parameter values exist such that the induced map (37) is well-defined in any finite dimension. Here we have chosen the parameters

$$
\begin{aligned}
&a = -1.8, \quad b_1 = -1.4, \quad b_2 = -1.4, \\
&b_r = 0.05, \ r = 3, \dots, 100, \\
&\alpha_1 = 0.2, \quad \alpha_2 = 0.8, \\
&\alpha_r = -0.0005, \ r = 3, \dots, 100, \quad \mu = 1,
\end{aligned}
\tag{40}
$$

with initial condition

$$z_1 = -0.001, \quad z_2 = -0.005,$$
$$z_r = 0, \ r = 3, \dots, 100.$$

The figure also shows the two half lines that define $D_1 \cup D_2$ and the structure is similar to that of the example of Figure 6, as expected. Note that the magnitude of the α_i are significantly smaller than those used in (39); the solutions are unbounded if larger values are used. Again, 10000 iterates are shown after discarding 501 to avoid transients, and the same result is observed (a bounded attractor indistinguishable by eye) if 100000 iterates are used.

7. The curse of dimensionality

The phrase 'the curse of dimensionality' is used in numerical analysis to describe methods that work well in low dimensions but take an absurdly long time to apply in higher dimensions. We believe that the results above show that nonsmooth bifurcation theory suffers from a similar problem. To be more specific, the connection between grazing-sliding and border collisions shows that complexity in the border collision normal form – in particular the fact that the number of different types of attractor that can exist – increases with dimension, so new possible dynamic behaviour arise as the dimension of the problem increases. This is in marked contrast to smooth bifurcation theory where, for local bifurcations for example, the dimension of the bifurcating system can be reduced to the dimension of the centre eigenspace, which will be one or two dimensions generically.

We shall illustrate this increasing complexity with a simple example, taking the matrices in (4) as

$$A_L = \begin{pmatrix} 0 & 1 & 0 & \ldots & 0 & 0 \\ 0 & 0 & 1 & \ldots & 0 & 0 \\ \vdots & \vdots & \vdots & \vdots & \vdots & \vdots \\ 0 & 0 & 0 & \ldots & 0 & 1 \\ 2 & 0 & 0 & \ldots & 0 & 0 \end{pmatrix} \tag{41}$$

and

$$A_R = \begin{pmatrix} 0 & 1 & 0 & \ldots & 0 & 0 \\ 0 & 0 & 1 & \ldots & 0 & 0 \\ \vdots & \vdots & \vdots & \vdots & \vdots & \vdots \\ 0 & 0 & 0 & \ldots & 0 & 1 \\ -2 & 0 & 0 & \ldots & 0 & 0 \end{pmatrix} \tag{42}$$

and letting $\nu = 1$, so the constant term in the border collision normal form is

$$(1, 0, 0, \ldots, 0, 0)^T. \tag{43}$$

Theorem 8 *Consider the m-dimensional border collision normal form with A_L and A_R given by (41), (42) and $\nu = 1$. Then there is an invariant m-dimensional hypercube $\mathcal{C}$ such that: (a) the Lebesgue measure is an invariant measure on $\mathcal{C}$; (b) the Lyapunov exponent of almost all points is positive on $\mathcal{C}$; (c) periodic orbits are dense in $\mathcal{C}$; (d) there is topological transitivity on $\mathcal{C}$; and (e) the map has sensitive dependence on initial conditions on $\mathcal{C}$.*

Proof: Let $\mathcal{C}$ be the hypercube with 2^m vertices $(u, v_2, \ldots, v_m)$ with $u \in \{-1, +1\}$ and $v_k \in \{-2, 0\}$, $k = 2, \ldots, m$. The discontinuity surface $z = 0$ divides $\mathcal{C}$ into two cubes, $\mathcal{C}_0$ in $z \leq 0$ and $\mathcal{C}_1$ in $z \geq 0$, so $\mathcal{C}_0$ has vertices $(u_0, v_2, \ldots, v_m)$ with $u_0 \in \{-1, 0\}$ and v_k as before, and $\mathcal{C}_1$ has vertices $(u_1, v_2, \ldots, v_m)$ with $u_1 \in \{0, +1\}$.

We will show that $F(\mathcal{C}_r) = \mathcal{C}$ for $r = 0, 1$, (we omit the parameter from F since we have set $\nu = 1$), by looking at the action of the map on the vertices (since the map is affine, if the vertices of $\mathcal{C}_r$ are mapped to those of $\mathcal{C}$, then the whole of $\mathcal{C}_r$ maps to $\mathcal{C}$).

Consider $\mathcal{C}_0$. The image of $(u_0, v_2, \ldots, v_m)$ is

$$(v_2 + 1, v_3, \ldots, v_m, 2u_0) \tag{44}$$

and since $v_2 \in \{-2, 0\}$, $v_2 + 1 \in \{-1, 1\}$, and v_3 to v_m are each in $\{-2, 0\}$. Finally, $2u_0 \in \{-2, 0\}$ as $u_0 \in \{-1, 0\}$ and this shows that vertices of $\mathcal{C}_0$ map to vertices of $\mathcal{C}$, clearly on a one-to-one basis, and hence $F(\mathcal{C}_0) = \mathcal{C}$. The argument for $\mathcal{C}_1$ is similar.

This establishes that $\mathcal{C} = \mathcal{C}_0 \cup \mathcal{C}_1$ is invariant and $F(\mathcal{C}_r) = \mathcal{C}$, $r = 0, 1$.

(a) Invariance of Lebesgue measure

First note that the modulus of the determinant of the linear part of the map describes how volumes (Lebesgue measure, ℓ) is changed, so if B is a measurable set in $x > 0$ or in $x < 0$ then $\ell(F(B)) = 2\ell(B)$.

Since $F(\mathcal{C}_r) = \mathcal{C}$, $r = 0, 1$, for any measurable $B \subset \mathcal{C}$ there exist $P_i \in \mathcal{C}_i$, $i = 0, 1$ such that $F(P_i) = B$ and $\ell(B) = 2\ell(P_i)$. In other words

$$\ell(B) = \ell(P_0) + \ell(P_1) = F^{-1}(B)$$

which is the condition for a measure to be invariant under F.

(b) Positive Lyapunov exponents

This is a simple calculation. Iterating the relation (44) n times (bearing in mind that the coefficient 2 could be either plus or minus two in the general case) shows that for a general point $\mathbf{x} = (x_1, x_2, \ldots, x_n)$

$$F^m(\mathbf{x}) = \begin{pmatrix} 1 + \sigma_1 2 x_1 \\ \sigma_2 2(1 + x_2) \\ \vdots \\ \sigma_m 2(1 + x_m) \end{pmatrix}$$

where $\sigma_k \in \{-1, +1\}$. Hence the linear part (the Jacobian) of the mth iterate of the map is

$$2\mathrm{diag}(\sigma_1, \sigma_2, \ldots, \sigma_m)$$

and hence every point in $\mathcal{C}$ has m Lyapunov exponents equal to $\frac{1}{m} \log 2$. (Note that this could be deduced using the Cayley-Hamilton Theorem and the fact that the characteristic equation of the linear parts of the map are $\lambda^m \pm 2 = 0$.)

(c-e) Locally eventually onto (LEO)

We shall prove the final three statements using a property called locally eventually onto [13]. The map F is LEO on $\mathcal{C}$ if for any open set $B \subset \mathcal{C}$ there exists $U \subset B$ and $m > 0$ such that $F^m(U) = \mathcal{C}$ and F^m is a homeomorphism on U. This clearly implies that a map is topologically transitive (i.e. for all open U, V there exists $m > 0$ such

that $F^m(U) \cap V \neq \emptyset$) and has periodic orbits dense, and this is enough to guarantee sensitive dependence on initial conditions.

By being a little more careful about the calculation leading to (44) we can show that if $\mathbf{x} = (x_1, x_2, \ldots, x_m)$ then $F^n(\mathbf{x}) = (X_1, X_2, \ldots, X_m)$ with

$$X_1 = \begin{cases} 1 - 2x_1 & \text{if } x_1 > 0 \\ 1 + 2x_1 & \text{if } x_1 < 0 \end{cases} \tag{45}$$

and for $k = 2, \ldots, m$,

$$X_k = \begin{cases} -2(1 + x_k) & \text{if } 1 + x_k > 0 \\ 2(1 + x_k) & \text{if } 1 + x_k < 0 \end{cases}. \tag{46}$$

In other words, both the coordinates decouple and satisfy a rescaled tent map for the mth iterate; with the tent map defined on $[-1, 1]$ for x_1 and $[-2, 0]$ for the other coordinates.

The tent map T clearly satisfies the LEO property, and if U is such that $T^m(U)$ covers the interval on which it is defined and is a homeomorphism, then for any $M > m$ there exists $U_M \in U$ such that $T^M(U_M)$ covers the interval on which the tent map is defined and is a homeomorphism.

Now consider an open set $B \subset \mathcal{C}$. Then this clearly contains a rectangle $I_1 \times \ldots \times I_m$ with $I_1 \subset [-1, 1]$ and $i_k \subset [-2, 0]$, $k = 2, \ldots, m$. Each of these contains an interval on which the corresponding tent map is LEO, and by taking the maximum of the iterates used, there are intervals V_j, $j = 1, \ldots, m$ and $N > 0$ such that the Nth iterate of the appropriate tent map has the LEO property (with the same N for all j). Hence by definition if $V = V_1 \times \ldots \times V_m$ then

$$F^{mN}(V) = \mathcal{C} \quad \text{and} \quad F^{MN}|V \text{ is a homeomorphism}$$

so F is LEO on $\mathcal{C}$.

□

Of course, $\mathcal{C}$ is not an attractor in the sense of the existence of an attracting neighbourhood, but like the logistic map with parameter equal to 4, $f(x) = 4x(1 - x)$, points outside the region tend to infinity. On the other hand it does 'attract' all points inside it and has the same dimension as the ambient space. By a small perturbation this can be made into a more conventional attractor, but we do not consider this more technical issue here.

This example can be modified to prove the existence of k dimensional attractors for all $k \in \mathbb{N}$, $k \leq m$.

Theorem 9 *For each $k \in \mathbb{N}$, $k \leq m$, there exist parameters of the m-dimensional border collision map (1) with an invariant set of dimension k and if $k \neq 0$ then the invariant set has the properties (a)-(e) described in Theorem 8 in the k non-trivial dimensions of the invariant set.*

Proof: The examples given below cannot be written in border collision normal form, though they are border collision maps and hence apply to border collision bifurcations.

If $k = 0$ then we need only to choose a map with a stable fixed point in the appropriate half-plane, so this is easy.

Suppose $k > 0$. Consider the piecewise affine map for $\mathbf{x} = (x_1, \ldots, x_m) \in \mathbb{R}^n$ defined by

$$\mathbf{x}_{j+1} = \begin{cases} B_L \mathbf{x}_j + \mathbf{b} & \text{if } x_1 \le 0 \\ B_R \mathbf{x}_j + \mathbf{b} & \text{if } x_1 > 0 \end{cases} \tag{47}$$

with

$$\mathbf{b}^T = (1, 0, \ldots, 0)$$

and

$$B_K = \begin{pmatrix} 0 & 1 & \ldots & 0 & 0 & \ldots & 0 \\ 0 & 0 & \ldots & 0 & 0 & \ldots & 0 \\ \vdots & \vdots & \vdots & \vdots & \vdots & \vdots & \vdots \\ 0 & 0 & \ldots & 1 & 0 & \ldots & 0 \\ 2\sigma_K & 0 & \ldots & 0 & 0 & \ldots & 0 \\ 0 & 0 & \ldots & 0 & q_1 & \ldots & 0 \\ \vdots & \vdots & \vdots & \vdots & \vdots & \ddots & \vdots \\ 0 & 0 & \ldots & 0 & 0 & \ldots & q_{m-k} \end{pmatrix} \tag{48}$$

$(K = R, L)$ with $\sigma_R = -1$, $\sigma_L = +1$ and $|q_r| < 1$, $1 \le r \le m - k$. So B_k has a $k \times k$ block with the same structure as (41) or (42) and an $(m - k) \times (m - k)$ block which is diagonal and the diagonal components with modulus less than one. Thus the second $m - k$ components of $\mathbf{x}$ decay to zero exponentially, whilst the behaviour of the first k components is as described in Theorem 8. Note that if $k = 1$ the dynamics in x_1 is determined by the tent map (as the x_2 component tends to zero). $\qquad \square$

8. Conclusion

We have shown how the border collision normal form in $n - 2$ dimensions arises naturally in the linearised model of the grazing-sliding bifurcation for flows in $n \ge 4$ dimensions (note that the equivalent result in three dimensions, where the one-dimensional border collision normal form is a continuous piecewise linear map, was been described in [11, 12]). We have also given examples of this correspondence with $n = 4$. Note that we have not shown that all possible border collision normal forms can arise this way (indeed we believe this cannot be the case in general, and this is certainly not the case if $n = 3$ [12]). For $n > 4$ we have shown examples in 100 dimensions which certainly suggest that the connection between the border collision and grazing-sliding bifurcations holds for arbitrary (finite) dimension.

In the final section we have shown that the border collision maps in m dimensions has parameters for which there is an attractor with topological dimension k for all $k =$

$0, 1, 2, \ldots, m$, and this, together with the possible link to grazing-sliding bifurcations, suggest that dimensionality poses a problem for nonsmooth bifurcation theory.

To simplify the preliminary description of grazing-sliding, we began by assuming a periodic orbit that formed a single connected path on one side of the switching surface (i.e. $y \geq 0$). The analysis in this paper, however, applies equally if the orbit intersects the switching surface far from the grazing point, so long as it does so transversally, and involves only crossing or attracting sliding, (but not repelling sliding, which involves forward time ambiguity of solutions, a different matter altogether, see e.g. [15]). A segment of sliding far from the grazing point has the effect of reducing the rank of the Jacobian of the global return map P_Π by one. In the observer canonical normal form this means setting the determinant of the Jacobian, the parameter b_{n-2} in (29) (up to a sign), to zero. Following the ensuing analysis in Section 5 with $b_{n-2} = 0$ suggests no significant effect on the border collision normal form, and therefore no obvious effect on the attractors permitted by it.

This paper leaves a number of different questions unanswered about the detail and multiplicity of stable solutions. However, the analysis simplifies some aspects of nonsmooth bifurcation theory by showing how two hitherto separate problems are connected, whilst at the same time complicating other aspects of the theory by pointing out the possible curse of dimensionality inherent in the description of bifurcating solutions.

References

[1] R. Bellman (2003). Dynamic Programming, Dover.

[2] A. Colombo, M. di Bernardo, S. J. Hogan, M. R. Jeffrey (2012) Bifurcations of piecewise smooth flows: perspectives, methodologies and open problems, Physica D, **241**, 1845–1860.

[3] M. di Bernardo (2003) Normal forms of border collision in high dimensional non-smooth maps, Proceedings IEEE ISCAS 2003, **3**, 76–79.

[4] M. di Bernardo, C. Budd, A.R. Champneys, P. Kowalczyk (2008) *Piecewise-smooth Dynamical Systems Theory and Applications*, Applied Mathematical Sciences, Vol. 163, Springer, London.

[5] M. di Bernardo, P. Kowalczyk, and A. B. Nordmark (2002) Bifurcations of dynamical systems with sliding: derivation of normal-form mappings, Physica D, **170**, 175–205.

[6] M. di Bernardo, U. Montanaro, and S. Santini (2011) Canonical Forms of Generic Piecewise Linear Continuous Systems, IEEE Trans. Automatic Control, **56** 1911–1915.

[7] J. Buzzi (1999) Absolutely continuous invariant measures for generic multi-dimensional piecewise affine expanding maps, *Int. J. Bifn. & Chaos* **9** 1743–1750.

[8] J. Buzzi (2001) Thermodynamic formalism for piecewise invertible maps: Absolutely continuous invariant measures as equilibrium states, in *Smooth Ergodic Theory and Its Applications*, eds. A. Kaotok, R. de la Llave, Y. Pesin and H. Weiss, AMS Proc. Symp. Pure Math. **69**, 749–784.

[9] A. F. Filippov (1988) *Differential Equations with Discontinuous Righthand Sides*, Kluwer Academic Publishers, Dortrecht.

[10] P. Glendinning (2013) Attractors with dimension n for open sets of parameter space in the n-dimensional border collision normal form, preprint, University of Manchester (MIMS Eprints).

[11] P. Glendinning, P. Kowalczyk and A.B. Nordmark (2012) Attractors near grazing-sliding bifurcations, to appear, Nonlinearity.

[12] P. Glendinning, P. Kowalczyk and A.B. Nordmark (2012) Attractors of three-dimensional grazing-sliding bifurcations modelled by two-branch maps, preprint, University of Manchester.

[13] P. Glendinning and C.H. Wong (2011) Two-dimensional attractors in the border-collision normal form, Nonlinearity **24** 995–1010.

[14] J. Guckenheimer and P. Holmes (1983) Nonlinear oscillations, dynamical systems, and bifurcations of vector fields, Springer, New York.

[15] M. R. Jeffrey (2011) Non-determinism in the limit of nonsmooth dynamics, Physical Review Letters, **106** 254103:1-4.

[16] Yu. A. Kuznetsov and S. Rinaldi and A. Gragnani (2002) One-parameter Bifurcations in Planar Filippov Systems, Int. J. Bifurcation and Chaos, **13** 2157–2188.

[17] C. Mira, L. Gardini, A. Barugola and J.C. Cathala (1996) *Chaotic Dynamics in Two-Dimensional Noninvertible Maps*, World Scientific, Singapore.

[18] H.E. Nusse and J.A. Yorke (1992) Border-collision bifurcation including 'period two to period three' for piecewise-smooth systems, Physica D, **57** 39-57.

[19] M. Tsujii (2001) Abolutely continuous invariant measures for expanding piecewise linear maps, *Invent. Math.* **143** 349–373

Appendix A. Proof of transformation results

Consider the n-dimensional system of piecewise smooth ordinary differential equations (5). Let there exist a periodic orbit in $h > 0$ that grazes the switching surface, $h = 0$, at the origin $(x, y, \underline{z}) = 0$ when $\mu = 0$. Without loss of generality this can be described as follows. Let $x = 0$ define a Poincaré section Π on which we define a return map $P_\Pi(x, y, \underline{z}; \mu)$, with a fixed point $P_\Pi(0, 0, \underline{0}; 0) = 0$. Choose y so that the switching surface lies at $y = 0$. We require that the periodic orbit ceases grazing when μ varies, so

$$\left. \frac{\partial(P \cdot \nabla h)}{\partial \mu} \right|_{(x,y,\underline{z};\mu)=(0,0,\underline{0};0)} \neq 0. \tag{A.1}$$

Let $\mathbf{y}$ be the column vector with components $(y, z_1, z_2, ..., z_{n-2})$. The linear approximation of P_Π can be written as

$$P_\Pi(\mathbf{y}) = \Lambda \mathbf{y} + \mu \mathbf{b}, \tag{A.2}$$

where $\mathbf{b}$ and Λ are $(n - 1)$ dimensional vectors and square matrices respectively.

For grazing to occur, there must be a tangency between the vector field f_+ and the switching surface $y = 0$ at the origin, meaning

$$h = f_+ \cdot \nabla h = 0, \quad \text{at} \quad (x, y, \underline{z}; \mu) = (0, 0, \underline{0}; 0), \tag{A.3}$$

where ∇h is the gradient of h in the coordinates $x, y, \underline{z}$. The vector field f_+ must be curving quadratically away from $y = 0$, while f_- must be pointing towards $y = 0$, so $f_+ \cdot \nabla(f_+ \cdot \nabla h)$ and $f_- \cdot \nabla h$ must be positive at $(x, y, \underline{z}; \mu) = (0, 0, \underline{0}; 0)$.

When μ is nonzero two things can happen, either the orbit given by the fixed point of P_Π lifts into the region $y > 0$, or it dips into the region $y < 0$. In the latter case the

map P_Π is no longer valid because the orbit it descibes contacts the switching surface. A Poincaré Discontinuity Mapping (see [5]), denoted by P_{DM}, applies the necessary correction to P_Π.

A discontinuity mapping takes account of dynamics that takes place on the switching surface $y = 0$, in this case in the neighbourhood of a grazing point. The flow crosses from $y < 0$ to $y > 0$ in the region

$$\{(x, y, \underline{z}) \in \Sigma : \ x < 0, \ y = 0\}. \tag{A.4}$$

In the complementary region

$$\{(x, y, \underline{z}) \in \Sigma : \ x > 0, \ y = 0\}, \tag{A.5}$$

f_+ and f_- both point towards $y = 0$, confining the flow to slide along inside the switching surface, as described in any standard text on piecewise-smooth flows (or *Filippov systems*), e.g. [4]. The sliding vector field is given by

$$(\dot{x}, 0, \dot{\underline{z}}) = f_s(x, \underline{z}; \mu) \quad \text{for} \quad (x, 0, \underline{z}) \in \Sigma_s, \tag{A.6}$$

where

$$f_s := \alpha f_+ + (1 - \alpha) f_-, \qquad \alpha = \frac{f_-^{(y)}}{f_-^{(y)} - f_+^{(y)}}, \tag{A.7}$$

as defined by Filippov [9], where $p^{(q)} = p \cdot \nabla q$ denotes the q component of p.

The Poincaré discontinuity mapping associated with the periodic orbit described above is that associated with a grazing-sliding bifurcation, with linear approximation derived in [5] given by

$$P_{DM}(\mathbf{y}) = \mathbf{y} - \begin{cases} 0 & \text{if} \ \ y > 0, \\ y\,\mathbf{k}(\mathbf{0}) & \text{if} \ \ y < 0, \end{cases} \tag{A.8}$$

in terms of the function

$$\mathbf{k} = \begin{pmatrix} 1 \\ \underline{c} \end{pmatrix} = \begin{pmatrix} 1 \\ \dfrac{f_-^{(\underline{z})}}{f_-^{(y)}} + \dfrac{f_{+,y}^{(y)} f_-^{(y)} + f_{+,\underline{z}}^{(y)} \cdot f_-^{(\underline{z})}}{f_{+,\underline{z}}^{(y)} \cdot f_+^{(\underline{z})}} f_+^{(\underline{z})} \end{pmatrix}. \tag{A.9}$$

For conciseness let us define

$$\underline{c}_0 := \underline{c}(\mathbf{0}) \qquad \text{and} \qquad C := \begin{pmatrix} 0 & \underline{0}^T \\ \underline{c}_0 & \underline{\underline{1}} \end{pmatrix}, \tag{A.10}$$

in terms of which we can then write

$$P_{DM}(\mathbf{y}) = \begin{cases} \mathbf{y} & \text{if} \ \ y > 0, \\ C\mathbf{y} & \text{if} \ \ y < 0. \end{cases} \tag{A.11}$$

With these preliminaries we now prove the transformation results from Section 5, namely Lemmas 4, 5, 6, and Corollary 7.

Proof of Lemma 4:

The linearization of the return map on Π in $y > 0$ can be generally written as

$$\mathbf{y}' = M\mathbf{y} + \mathbf{r}, \tag{A.12}$$

where $\mathbf{r}$ is an $n-1$ dimensional column vector, and M is an $(n-1) \times (n-1)$ matrix. We neglect higher order terms. Let $\mathbf{s} = (1, 0, 0, ...)$ and

$$O = \begin{pmatrix} \mathbf{s} \\ \mathbf{s}M \\ \mathbf{s}M^2 \\ \vdots \\ \mathbf{s}M^{n-2} \end{pmatrix} \qquad T = \begin{pmatrix} 1 & 0 & 0 & 0 & ... \\ t_1 & 1 & 0 & 0 & ... \\ t_2 & t_1 & 1 & 0 & ... \\ \vdots & \vdots & \vdots & \vdots & ... \\ t_{n-2} & t_{n-3} & t_{n-4} & ... & 1 \end{pmatrix}, \qquad (A.13)$$

where t_i, $i = 1, ..., n-1$, are the coefficients of the characteristic polynomial of M, for example t_1 is the trace and $(-1)^n t_{n-1}$ (which doesn't appear in T) is the determinant of M. If O is nonsingular, we can define another matrix $W = TO$ and a new coordinate $\tilde{\mathbf{y}} = W\mathbf{y}$, so that

$$\mathbf{y}' = \tilde{M}\mathbf{y} + \tilde{\mathbf{r}}, \qquad (A.14)$$

where $\tilde{M} = WMW^{-1}$ and $\tilde{\mathbf{r}} = W\tilde{\mathbf{r}}$. The first row of W is $(1, 0, 0, ...)$ so the transformation does not touch the first component of $\mathbf{y}$ (the coordinate y which is orthogonal to the switching surface). As proven in [6], $\tilde{M}$ then has the convenient form

$$\tilde{M} = \begin{pmatrix} a & 1 & 0 & 0 & ... \\ b_1 & 0 & 1 & 0 & ... \\ b_2 & 0 & 0 & 1 & ... \\ \vdots & . & . & . & ... \\ b_{n-2} & 0 & 0 & ... & 0 \end{pmatrix}, \qquad (A.15)$$

where we replace the symbols $(t_1, t_2, t_3, ..., t_{n-1})$ with $(a, b_1, b_2, ..., b_{n-2})$. A simple translation sends the components of $\tilde{\mathbf{r}}$ to $(\mu, 0, 0, ...)$. This is done by replacing $\underline{z}$ with $\underline{z} - Q\tilde{\mathbf{r}}$ and defining $\mu = r_1 - (1, 0, 0, ...)Q\tilde{\mathbf{r}}$, where Q is the upper triangular matrix

$$\begin{pmatrix} +1 & -1 & +1 & -1 & ... \\ 0 & +1 & -1 & +1 & ... \\ \vdots & \vdots & \vdots & \vdots & ... \\ 0 & 0 & 0 & ... & +1 \end{pmatrix},$$

which gives the result as stated.

□

Proof of Lemma 5:
The form of the Poincaré Discontinuity Map P_{DM} is not changed by the transformations performed in the previous lemma, because any transformation matrix (in particular W in the proof above) in which the first row is $(1, 0, 0, ...)$, only transforms the value of $\underline{\alpha}$ in (30), as is easily shown.

□

Proof of Lemma 6:
If $\underline{Z} \in D_1$ then the first component of $F(\underline{Z}; \mu) = F_1(\underline{Z}; \mu)$ is $\alpha_1 Z_1 + Z_2$, and so $F_1(\underline{Z}; \mu) \in \{\underline{Z} \in \mathbb{R}^{n-2} \mid Z_1 \le 0\}$ by the definition of D_1, and $F^2(\underline{Z}; \mu) = F(F_1(\underline{Z}; \mu); \mu) = F_1^2(\underline{Z}; \mu)$,

which is well defined for $\underline{Z} \in D_1$ and is found by direct calculation. In particular, continuity is provided by

$$F_1^2(0, Z_2, ...Z_{n-2}; \mu) = F_2(0, Z_2, ..., Z_{n-2}; \mu)$$
$$= (\ \alpha_1 Z_2 + Z_3 + \mu \ , \ \alpha_2 Z_2 + Z_4 + \mu, \alpha_3 Z_2 + Z_5 + \mu, \ ... \ ,$$
$$\alpha_{n-4} Z_2 + Z_{n-2} + \mu, \ \alpha_{n-3} Z_2 + \mu, \ \alpha_{n-2} Z_2 + \mu \ ),$$

and therefore since F_1^2 and F_2 are continuous at $Z_1 = 0$, G is continuous.

$\square$

Proof of Corollary 7:
The border collision normal form is obtained as follows. Let $\underline{s} = (1, 0, 0, ...)$, $M_R = \frac{d}{d\underline{Z}} F_2$, and

$$O_R = \begin{pmatrix} \underline{s} \\ \underline{s} M_R \\ \underline{s} M_R^2 \\ \vdots \\ \underline{s} M_R^{n-3} \end{pmatrix} \qquad P_R = \begin{pmatrix} 1 & 0 & 0 & 0 & ... \\ r_1 & 1 & 0 & 0 & ... \\ r_2 & r_1 & 1 & 0 & ... \\ \vdots & \vdots & \vdots & \vdots & ... \\ r_{n-3} & r_{n-4} & r_{n-5} & ... & 1 \end{pmatrix}, \qquad \text{(A.16)}$$

where r_i are the coefficients of the characteristic polynomial of M_R, for example r_1 is the trace and $(-1)^n r_{n-2}$ is the determinant of M_R. As shown in [6], if O_R is nonsingular, we can define another matrix $W_R = P_R O_R$ and a new coordinate $\underline{Y} = W_R \underline{Z}$, so that the map G is specified by the matrices $A_L = W_R M_L W_R^{-1}$ and $A_R = W_R M_R W_R^{-1}$, which are in the border collision normal form

$$A_L = \begin{pmatrix} l_1 & 1 & 0 & 0 & ... \\ l_2 & 0 & 1 & 0 & ... \\ l_3 & 0 & 0 & 1 & ... \\ \vdots & . & . & . & ... \\ l_{n-2} & 0 & 0 & ... & 0 \end{pmatrix}, \qquad \text{(A.17)}$$

$$A_R = \begin{pmatrix} r_1 & 1 & 0 & 0 & ... \\ r_2 & 0 & 1 & 0 & ... \\ r_3 & 0 & 0 & 1 & ... \\ \vdots & . & . & . & ... \\ r_{n-2} & 0 & 0 & ... & 0 \end{pmatrix} \qquad \text{(A.18)}$$

where r_i and l_i are the coefficients of the characteristic polynomials of $M_R = \frac{d}{d\underline{Z}} F_2$ and $M_L = \frac{d}{d\underline{Z}} F_1^2$, respectively.

$\square$